Institute of Paper Science and Technology
500 10th Street, NW
Atlanta, GA 30318-5794

Kinetics of the Titanate Causticization Reactions in a Potassium-Based Process

by
Luis Holing Ho
Candidate for Master's Degree

Advisor: Dr. Jeff Empie

April 16, 2004

Table of Contents

Abstract

The objective of this study was to model the kinetics of direct causticization of potassium-based chemical using titanium dioxide, TiO_2. The starting materials were K_2CO_3 and TiO_2. Potassium chemical was used because there is an indication that potassium carbonate, K_2CO_3, might offer benefits over sodium carbonate, Na_2CO_3, such as the elimination of potassium build-up in sodium-based pulping.

Experiments were run at six different temperatures. Half were below potassium carbonate's melting point while the other half were above. Reaction rates and conversions increased with temperature, and the maximum conversion achieved was 0.90.

Several kinetic models were fitted to the data. Valensi-Carter showed a good fit for the solid-solid reaction, while ash diffusion control model was chosen to describe the solid-liquid reaction with TiO_2 stayed in solid phase.

The samples from the heated experiments were then leached with water to produce KOH. The amount of KOH was found to increase with temperature. It implied that more $4K_2O{\cdot}5TiO_2$ was produced at higher temperatures.

Reacting K_2CO_3 with $K_2O{\cdot}3TiO_2$ might interest industry more because TiO_2 is added to the recovery system as a make up only. The models used did not show good fits for the whole conversions; therefore, additional study should be done to develop a model that could describe low conversions as well as high conversions.

List of Figures

List of Tables

Introduction

The kraft pulping process has been based on sodium chemicals (NaOH and Na_2S). However, limited laboratory studies show that kraft pulps can be produced effectively using potassium hydroxide, KOH, and potassium sulfide, K_2S. In fact, there are some indications that potassium-based alkali might actually improve pulping rate and quality [1].

The conventional recovery process has several drawbacks, including high capital cost, low energy produced efficiency, and limited operation variability. These drawbacks have led to the research and development of alternatives such as different gasification and causticization processes, e.g. direct caustization using titanate. Such a process would replace the recovery boiler by a gasifier and the conventional lime cycle by a titanate cycle with direct causticization in the gasifier.

In the titanate-based chemical recovery process for potassium-based pulping, potassium hydroxide is recovered by reacting potassium carbonate, K_2CO_3, with titanium dioxide, TiO_2, and leaching the titanate products with water. From an industry point of view, there is a greater interest to use potassium trititanate, $K_2O{\cdot}3TiO_2$, instead of titanium dioxide because the trititanate produced in the leaching step is recycled to the gasifier, while titanium dioxide is added to the gasifier as a make up chemical only. However, the trititanate is not available commercially.

This study proposed to analyze the effectiveness of using titanate as a causticizing agent in the potassium-based pulping process. The combination of a titanate based recovery with a potassium-based pulping process could lead to a more effective pulping and recovery process.

1. Literature Review

1.1. Potassium-Based Pulping

Alkaline pulp mills have used sodium chemicals in many processes including the kraft process. However, there are some problems associated with sodium-based pulping, with the main problem being potassium build up. Among non-process elements in the kraft recovery system, such as K, Cl, Al, Fe, Si, Mn, Mg, and Ca, potassium has the highest tendency to accumulate in an alkali cycle [2]. The potassium comes from wood chips because it is one of the components found in trees. The build-up problem has increased because potassium is very soluble in black, green, and white liquors. The amount of potassium can reach up to 10% in some mills and some efforts have been made to purge the build up, but they have not been successful [1].

Kraft black liquor recovery boilers have two main functions, to recover the inorganic cooking chemicals used in the pulping process, and to generate steam for the mill. Superheaters in the boiler are used to transfer heat from the flue gases to the saturated steam that has been relieved from the steam drum. As a result, the steam becomes superheated due to the increase in temperature [3].

Another problem that is associated with the presence of potassium in a sodium-based chemical pulping is unexpected shutdown on a black liquor recovery boiler. The shutdown will take place if corrosion occurs in the recovery boiler superheaters which are caused by melted deposits that reside in the recovery boiler. The melting point of the deposits decreases as the potassium content increases, as shown in Figure 1-1.

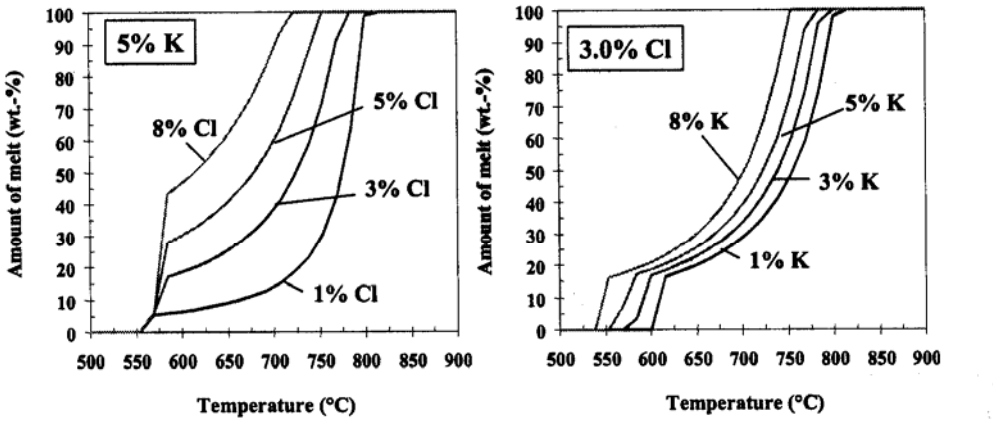

Figure 2. Effect of Cl (left) and K (right) content on the melting behavior of typical BLRB deposits.

Figure 1-1 Corrosion rate by varying Cl and K contents at different temperature [4].

One possible solution to the potassium build-up problem involves converting sodium-based pulping to potassium-based pulping. Some of the benefits that result from the conversion are [1]:

1. Elimination of low-melting sodium-potassium eutectics that aggravate plugging and corrosion in recovery boilers.
2. Increased pulping rates giving increased pulping capacity through existing equipment.
3. The possibility of an easier bleaching pulp.

A study on potassium-based pulping in comparison to sodium-based pulping has been reported [5]. Analysis was done to approximate the amount of potassium and sodium found in different tree species. Potassium was found to be greater than sodium by at least a factor of two.

The study also reported some advantages of the potassium-based pulping. First, it would have increased dissolution rates over sodium-based pulping. Second, a 2-3% increase in yield can be obtained, and, finally, faster lignin removal rate in the initial phase can be accomplished. As a result, no negative effects should be encountered as far as pulping characteristics are concerned.

1.2. Black Liquor Recovery Processes

Black liquor is a waste product from the manufacturing of pulp/paper. It contains almost all of the inorganic cooking chemicals along with the lignin and other organic matter separated from the wood during pulping in the digester. The lignin and other organic matter can be recovered from the black liquor by combustion process in the recovery boiler producing heat in the form of steam. The sodium chemicals can be converted to sodium hydroxide and sodium sulfide, i.e. white liquor, which is reused in the pulping process.

However, the conventional black liquor recovery has some major drawbacks, which are:

1. The dead load of sodium carbonate in the sodium cycle is substantial due to the unfavorable equilibrium of the causticizing reaction.
2. The lime kiln is the main consumer of external fuel in the pulp mill.
3. The ratio between electrical and heat energy produced in the recovery boiler is low.
4. The recovery boiler is associated with a risk of smelt-water explosions.
5. Recovery boiler capital cost is about $100 million.

Therefore, research has been done to find alternative black liquor recovery processes which can overcome these drawbacks. Gasification and alternative causticization processes have been suggested as the promising solutions.

1.2.1. Gasification Process

The black liquor gasification process converts the organic substances in the liquor into combustible gases and the inorganics into compounds suitable for regeneration of pulping chemicals. The result is a fuel gas which contains a large concentration of carbon monoxide (CO), hydrogen (H_2), and hydrogen sulfide (H_2S) in addition to CO_2, N_2, and H_2O. If complete carbon conversion can be achieved, the gasification process can be considered successful because carbon conversion influences energy conversion. A 10% drop in carbon conversion tends to decrease the net energy conversion by 6-7% [6].

In black liquor gasification, the gasification operates in a reducing environment, which is beneficial to the chemical recovery process. Sulfate reduction requires a

reducing environment to form sodium carbonate and sodium sulfide because carbon and sulfur tend to bind to sodium due to a lack of oxygen.

The gasification processes can be classified into two main groups:

1. Low temperature processes (<715^{o}C), where the inorganic salts are removed as dry solids.
2. High temperature processes (>900^{o}C), where an inorganic molten smelt is formed.

Comparisons of different gasification processes and conventional recovery technology have been made. Gasification processes have a capability of converting 18%-25% of the HHV (Higher Heating Value) in the black liquor into electrical power, while the capability of the conventional recovery technology only ranges from 10%-15% [6].

1.2.2. Causticization Processes

There are two different causticization processes, autocausticization and direct causticization. An amphoteric oxide is used in both processes as the causticization agent. If the oxide used is water soluble, the process is called autocausticization, and if the oxide used is insoluble in alkaline solutions, the process is called direct causticization.

1.2.2.1. Autocausticization

Three reactions occur in the autocausticization process (Reactions 1-1 to 1-3), and the possible water soluble amphoteric oxides that have been suggested are BO_3, P_2O_5, and SiO_2 [7-10]. The oxide will initially react with sodium carbonate in the autocausticization process (Reaction 1-1). The product of the first reaction is then dissolved in water (Reaction 1-2), and finally, protolysis occurs to produce sodium hydroxide, which can be used to produce white liquor (Reaction 1-3).

Causticization

$$Na_2CO_3\ (s) + n\ Y\ (s) \leftrightarrow Na_2Y_nO\ (s) + CO_2\ (g) \qquad \text{(Reaction 1-1)}$$

Where Y = amphoteric oxide

Dissolution

$$Na_2Y_nO\ (s) + H_2O \leftrightarrow Na_2H_2Y_nO_2\ (aq) \qquad \text{(Reaction 1-2)}$$

Protolysis

$$Na_2H_2Y_nO_2\ (aq) \leftrightarrow NaOH\ (aq) + n\ Y\ (aq) \qquad \text{(Reaction 1-3)}$$

Since the oxide is water soluble, it accompanies the cooking chemicals in the liquor cycle; therefore, it can be regarded as part of the cooking alkali. However, the presence of the oxide might change the characteristics of the white liquor, but these changes are not yet fully understood [11].

1.2.2.2. Direct Causticization

Two reaction steps are involved in forming sodium hydroxide in the direct causticization process (Reactions 1-4 and 1-5). The sodium carbonate used could be either in solid or liquid phase. Since the oxide used is insoluble in alkaline solutions, it can be precipitated from sodium hydroxide solutions during the dissolution stage and recycled to react further with sodium carbonate (Reactions 1-6). The causticizing agent used in this process is in the form of metal oxide (M_xO_y). The oxides proposed are iron oxide, titanium dioxide, alumina, and manganese oxide [7-10, 12].

General reaction

$$a\ Na_2CO_3 + b\ M_xO_y\ (s) \leftrightarrow aNa_2O{\cdot}bM_xO_y\ (s) + a\ CO_2\ (g) \qquad \text{(Reaction 1-4)}$$

Hydrolysis reaction

$$aNa_2O{\cdot}bM_xO_y\ (s) + (a+z)\ H_2O \leftrightarrow 2a\ NaOH\ (aq) + bM_xO_y{\cdot}z\ H_2O\ (s) \qquad \text{(Reaction 1-5)}$$

The precipitated causticizing agent can be separated from the white liquor and reused for direct causticization (Reaction 1-6).

$$a\ Na_2CO_3 + bM_xO_y{\cdot}z\ H_2O\ (s) \leftrightarrow aNa_2O{\cdot}\ bM_xO_y\ (s) + a\ CO_2\ (g) + z\ H_2O \qquad \text{(Reaction 1-6)}$$

Some advantages of the direct causticizing process as compared to the conventional causticizing process are:

1. Energy needed is reduced because of the elimination of the lime cycle.
2. High concentration of sodium hydroxide is obtained so the white liquor concentration can be controlled.
3. Dead load of sodium carbonate is greatly reduced because a high efficiency causticizing can be obtained.

However, there are also some possible disadvantages associated with the causticizing process, which need further investigation. The disadvantages are:

1. The cost of causticizing agents
2. Possible accumulation of non-process elements in the liquor cycle
3. Possible dead load of metal oxides in the oxide circulation system

Chemical equilibrium calculations were performed to select the best causticizing agent among three metal oxides, Fe_2O_3, Al_2O_3 and TiO_2. The only suitable causticization agent for kraft pulping system is TiO_2 [13]. Iron oxide was found to react with sodium sulfide, Na_2S, to form FeS, and Fe_2O_3 can easily be reduced to Fe and FeO by reducing agents such as C, H_2 and CO at temperatures as low as 50^oC. Therefore, Reaction 1-5 would not proceed and no sodium hydroxide would be obtained. The solubility behavior of the Al_2O_3 was found to make it unsuitable for direct causticization of kraft black liquor because some of its hydrates are soluble in white liquor.

The effectiveness of using manganese oxide, Mn_3O_4, as a direct causticizing agent has also been studied. The study confirmed that NaOH was obtained in a sulfur free environment. However, if Na_2S is present, it would reduce Mn_3O_4 to MnO [12].

Direct Causticization Using Titanate

As described earlier, titanium oxide (TiO_2) has been found to be the most promising direct causticizing agent for the kraft process. The reaction between sodium carbonate and titanium oxide may lead to the formation of different mixed oxide compounds such as $4\ Na_2O{\cdot}5TiO_2$, and $Na_2O{\cdot}3TiO_2$. A generalized form to present how these oxides are formed is shown below.

Causticization

$$a\ Na_2CO_3 + b\ TiO_2\,(s) \leftrightarrow aNa_2O{\cdot}bTiO_2\,(s) + a\ CO_2\ (g) \qquad \text{(Reaction 1-7)}$$

Hydrolysis

$$aNa_2O{\cdot}bTiO_2\,(s) + a\ H_2O \leftrightarrow 2a\ NaOH\ (aq) + b\ TiO_2\,(s) \qquad \text{(Reaction 1-8)}$$

However, the main reactions are considered to be:

Causticization

$$Na_2CO_3\,(s) + 3\ TiO_2\,(s) \leftrightarrow\ Na_2O{\cdot}3TiO_2\,(s) +\ CO_2\ (g) \qquad \text{(Reaction 1-9)}$$

$$\Delta H_{1123K} = 6.2\ \text{kJ/mol NaOH}$$

$$7\ Na_2CO_3\,(s) + 5\ (Na_2O{\cdot}3TiO_2)\,(s) \leftrightarrow 3\ (4Na_2O{\cdot}5TiO_2)\ (s) + 7\ CO_2\,(g)$$

(Reaction 1-10a)

$$\Delta H_{1123K} = 45\ \text{kJ/mol NaOH}$$

$$7\ Na_2CO_3\,(l) + 5\ (Na_2O{\cdot}3TiO_2)\,(s) \leftrightarrow 3\ (4Na_2O{\cdot}5TiO_2)\ (s) + 7\ CO_2\,(g)$$

(Reaction 1-10b)

$$\Delta H_{1123K} = 31\ \text{kJ/mol NaOH}$$

$$3\ (4Na_2O{\cdot}5TiO_2)\ (s) + 7\ H_2O \leftrightarrow 5\ (Na_2O{\cdot}3TiO_2)\,(s) + 14\ NaOH\ (aq) \qquad \text{(Reaction 1-11)}$$

$$\Delta H_{373K} = 7.6\ \text{kJ/mol NaOH}$$

Figure 1-2 shows the flow chart where these reactions occur during the process. Heavy black liquor is fed to a gasifier accompanied by recycled sodium tri-titanate, air or oxygen, and titanium dioxide (if needed). Reaction 1-9 will only occur if titanium dioxide is fed to the gasifier. Reaction 1-10 occurs in the gasifier with a suggested temperature of at least 840^{o}C to obtain a high reaction rate. Two streams leave the gasifier; one gaseous and one solid. The gas stream contains hydrogen sulphide among other gas products, and the solid stream contains sodium penta-titanate. The hydrogen sulphide is recovered in an absorption unit to obtain a sulfide rich white liquor; the gas products can be used to

produce electricity in a gas turbine. The solid stream goes to a leaching plant where the sodium penta-titanate reacts with water to form sodium hydroxide.

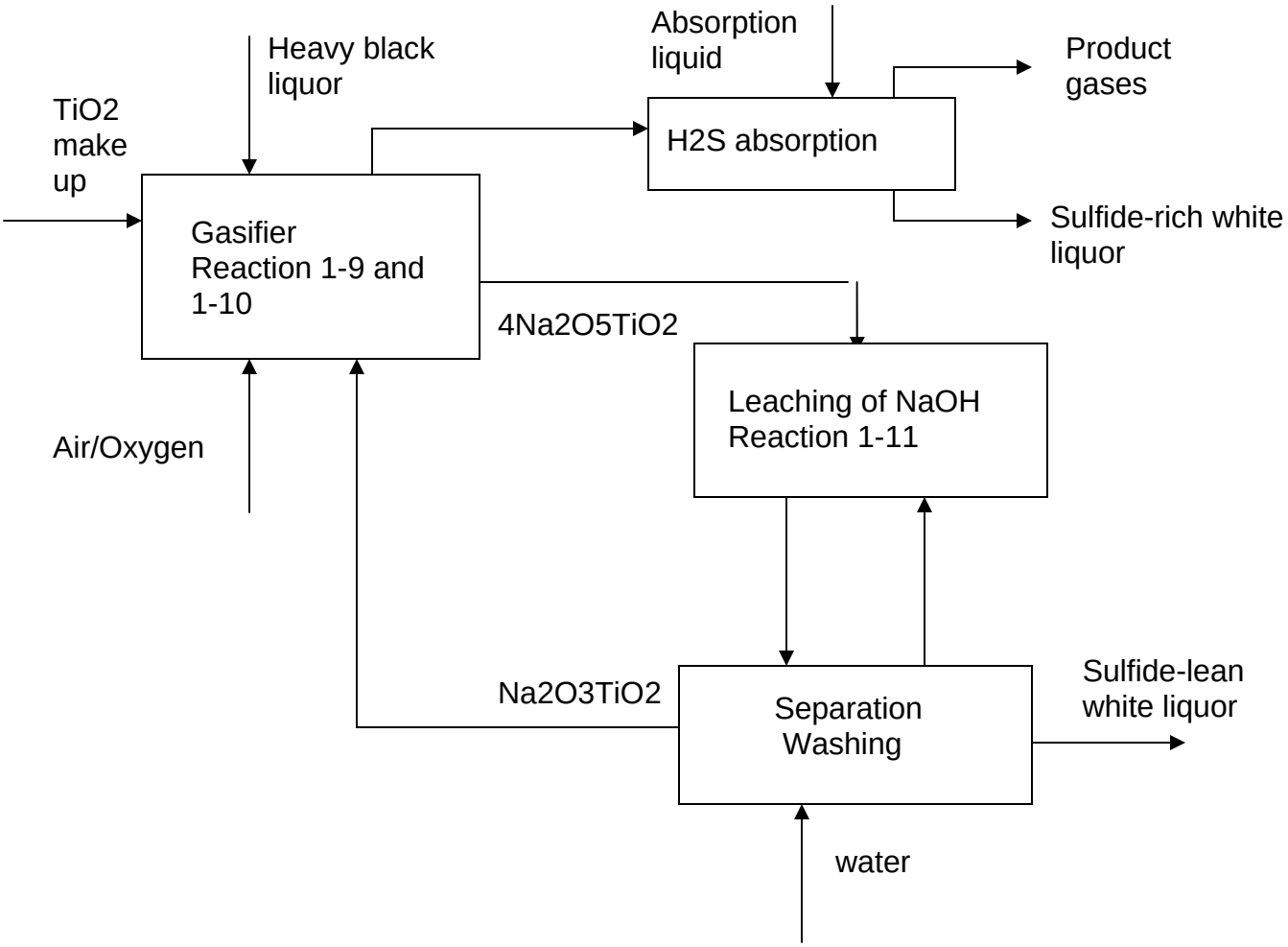

Figure 1-2. Gasification system with direct causticization using titanate [11].

Kinetic Study on the Direct Causticization

Most solid state reactions are controlled by mass transfer, i.e. the rate limiting step is diffusion of one or several reactants through the product layer to the other reactants. Studies of systems similar to that of potassium-titanates have shown diffusion controlled kinetics for solid-solid reaction and reaction controlled kinetics for solid-liquid reaction [10].

Solid-Solid Reaction

Some examples of commonly used models for solid-solid reactions are shown in Table 1-1. The most common models based on diffusion-controlled kinetics are the Jander model, the Ginstling-Brounshtein model, and the Valensi-Carter model. All of these models assume spherical particles and that surface diffusion rapidly covers reactant particles with a continuous product layer during the initial stages of the reaction. These models are often called "shrinking-core" models, i.e. it is assumed that there is a shrinking homogenous core of reactant surrounded by a homogenous shell of product. The Jander model is the simplest model, where the reacting spherical shell is approximated by a plane sheet when the diffusion equation is applied. In addition, the total radius of reacted and unreacted material is assumed to be constant throughout the reaction. Consequently, even if it is possible to fit the Jander model to experimental data, it is hardly possible to extrapolate the model to high conversions because the geometrical assumptions are, in this case, far from realistic. The Ginstling-Brounshtein model is based on diffusion through a spherical shell but assumes, as the Jander model, that the total radius of reacted and unreacted material is constant throughout the reaction. Furthermore, a model based on reaction controlled kinetics has been developed. It assumes that the reaction is not affected by any ash layer.

Solid-Liquid Reaction

Experiments might be carried out at a temperature at which one of the starting materials melts. As a result, several shrinking-core models that describe solid-liquid reaction are compiled in Table 1-2. The shringking-core models assume that there are five steps happen during reaction, as shown in Figure 1-3 [14]:

1. Diffusion of fluid reactant through the film layer
2. Diffusion of fluid reactant through the ash layer to the surface of the unreacted core
3. Reaction of the fluid reactant with solid at the surface
4. Diffusion of gaseous products through the ash layer
5. Diffusion of gaseous products through the film layer

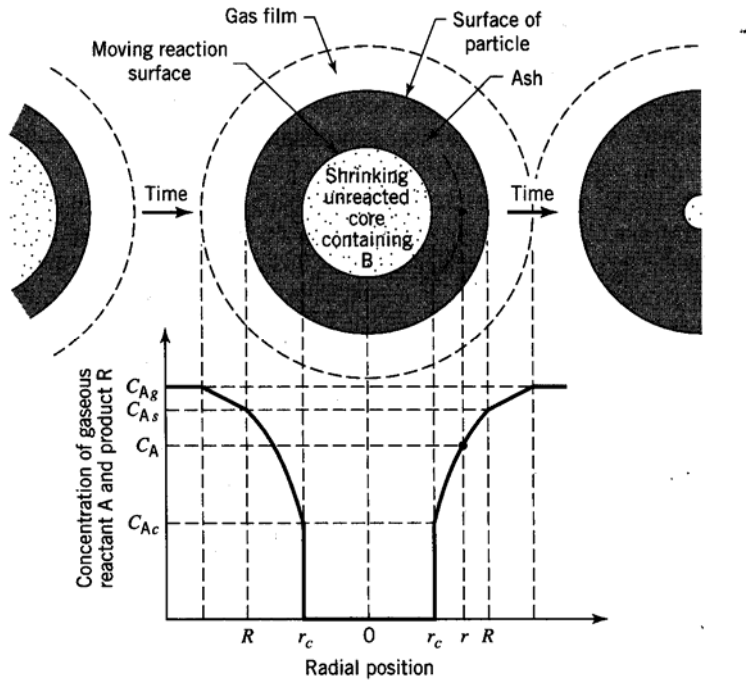

Figure 1-3. Solid-liquid reaction steps.

The first two models in Table 1-2 are film and ash diffusion control. Both models assume that the particle size is constant due to the presence of ash layer. In addition, a film layer is also present covering the ash layer. Therefore, the difference between the models is determined by the layer that controls the rate of reaction. Third is reaction control. The model is similar to phase boundary model from Table 1-1, but the unit is different for k. It assumes that the reaction is not affected by any ash layer; therefore, the rate is proportional to the available surface of unreacted core.

Table 1-1. Models used to describe solid-solid reactions. x is the degree of conversion ($0 \leq x \leq 1$), k the rate constant, t the time, z the volume of product formed per volume of reactant consumed, r the radius, and r_0 the initial radius of the sphere

MODEL	**RATE-CONTROLLING STEP**	**EQUATION (INTEGRATED)**	**SOURCE**
Jander	diffusion	$\frac{2k}{r_0^2}t = (1-(1-x)^{1/3})^2$	15
Ginstling-Brounshtein	diffusion	$\frac{2k}{r_0^2}t = 1 - \frac{2x}{3} - (1-x)^{2/3}$	15
Valensi-Carter	diffusion	$\frac{2(1-z)k}{r_0^2}t + z = (1+(z-1)x)^{2/3} + (z-1)(1-x)^{2/3}$	16
Phase-boundary spherical geometry	phase-boundary reaction	$\frac{k}{r_0}t = 1-(1-x)^{1/3}$	15

Table 1-2. Models used to describe solid-liquid reactions. x is the degree of conversion ($0 \leq x \leq 1$), k the rate constant, t the time, , and C_{Ao} the starting fluid.

MODEL	RATE-CONTROLLING STEP	EQUATION (INTEGRATED)	SOURCE
Film Diffusion Controls	diffusion	$\frac{t}{\tau} = x$ $\tau = \frac{4\rho_B R}{15 k C_A}$	14
Ash Diffusion Control	diffusion	$\frac{t}{\tau} = 1 - 3(1-x)^{2/3} + 2(1-x)$ $\tau = \frac{4\rho_B R^2}{30 D C_A}$	14
Reaction Controls	reaction	$\frac{t}{\tau} = 1 - (1-x)^{1/3}$ $\tau = \frac{4\rho_B R}{5 k C_{Ao}}$	14

Arrhenius' Law

The relationship between reaction rates and temperature is well presented by Arrhenius' law, Equation 1-1. The pre-exponential factor and activation energy could be obtained by plotting k vs. 1/T and adding an exponential trendline. High activation energies imply that the reactions are very temperature-sensitive [14].

$k = k_o \, EXP(-E_a/RT)$ Equation 1-1

where: k = Reaction constant (Unit depends on the type of reactions)
k_o = Pre-exponential factor (Similar unit with k)
E_a = Activation energy of the reaction (J/mol)
R = Gas Constant (J/mol.K)
T = Temperature (K)

2. Objectives

The direct causticizing process with titanate as the causticizing agent has been studied based on sodium-based pulping. However, there is an interest for using potassium-based pulping instead. Therefore, research is needed to study the performance of the direct causticizing process with titanate as the causticizing agent in a potassium-based pulping system.

The objectives to this study are as follow:

1. To react potassium carbonate and titanium dioxide according to Reaction 1-7 at high temperatures (700-950^{o}C).
2. To model the kinetic data obtained from the reaction.
3. To leach the product obtained from the reaction to measure KOH formation.

3. Research Scope

Chemicals used for this study were potassium carbonate and titanium dioxide. Their physical properties are shown in Table 3-1.

Table 3-1. Physical properties of the starting materials [17].

Properties	K_2CO_3	TiO_2
molecular weight (g/mol)	138.2	79.87
Melting Point (^{o}C)	891	1855
Density (g/mL)	2.29	4.26

Since switching from sodium-based pulping to potassium based pulping is still a challenging idea, equilibrium calculations were performed using the FactSage5.1 program. The program determines the equilibrium composition of a chemical system by minimizing the Gibbs free energy of the system.

Experiments were also carried out in a laboratory. A condition that was varied for the experiments was temperature. The results were then compared to the FactSage5.1 data.

3.1. Equilibrium Calculation

Equilibrium calculations were performed for K_2CO_3-TiO_2 reaction. The results gave an indication of what chemicals were present when equilibrium was reached at different temperatures.

3.2. Experimentation

Experiments were conducted in a hot furnace which is shown in Figure 3-1. A parameter that was evaluated was the influence of temperature on the reaction kinetics. Potassium carbonate has a melting point of 891^{o}C as shown in Table 3-1; therefore, three different temperatures below and above its melting point were studied, 700^{o}C, 750^{o}C, 800^{o}C, 900^{o}C, 925^{o}C, and 950^{o}C. These temperatures corresponded to the temperature range studied in the equilibrium calculations. To determine the causticizing efficiency, the solid product obtained from the reaction was leached with water and titrated with HCl to determine the amount of potassium hydroxide formed. Furthermore, particle size measurements and carbonate analyses were carried out to model the kinetics and estimate the reaction conversions, respectively.

3.2.1. Sample Preparation

The sample was prepared by dissolving potassium carbonate in distilled water. Titanium dioxide (size < 125 μm) was then added. The suspension was heated to its boiling point to evaporate the water while being stirred with a magnetic stirrer. When the concentration of solids in the suspension became very high and, consequently, the magnetic stirrer could not operate properly, the sample was put in a furnace (105^{o}C) to dry overnight. Finally, the dried sample was ground to a fine powder (size < 125 μm). The molar ratio used was TiO_2/K_2CO_3 = 5/4 in all of the experiments, which corresponds to the stoichiometric ratio as shown in Reaction 3-1.

$$5TiO_2 + 4K_2CO_3 \rightarrow 4K_2O{\cdot}5TiO_2 + 4\ CO_2 \qquad \text{Reaction 3-1}$$

3.2.2. Heating Procedure

The reaction was run in a furnace, shown in Figure 3-1. The temperature inside the furnace was measured by a thermocouple. A zirconium crucible was filled with 5 g of sample and placed inside the furnace above a ceramic tube. A weight balance which is put below the tube was used to measure the weight loss due to the release of CO_2. The measurements were taken for every 0.05 g of CO_2 that left the reactor until the weight stayed constant for significant amount of time. Conversions were then calculated based on weight loss using Equation 3-1.

$$X = \frac{\text{Accumulated Weight Loss (g)}}{\text{Theoretical Maximum Weight Loss (g)}} \qquad \text{Equation 3-1}$$

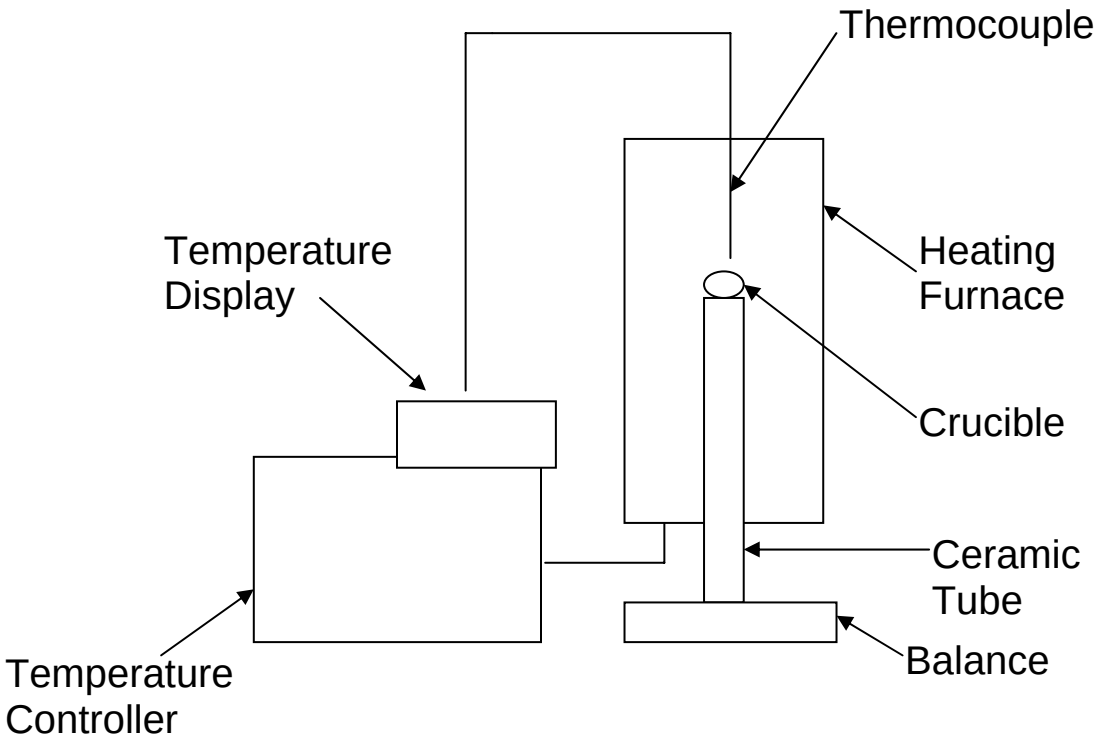

Figure 3-1. Heating furnace.

3.2.3. Leaching and Titrating

The analytical leaching of the samples were carried out in a 500 mL 3-necked flask equipped with a water-cooled condenser, a thermometer and a Pasteur pipette through which N_2 gas was bubbling through in order to eliminate air, as shown in Figure

3-2. The flask was filled with 100 mL of DI water and heated via an oil bath in order to bring the water to boil while being stirred with a magnetic stirrer. Evaporated water was condensed and refluxed back into the flask. When the water reached its boiling point, 1.000 g of the sample was added. The leaching time was determined to be 120 min from Figure 3-3 in order to ensure complete reaction.

After the leaching time had elapsed, the flask with the contents was removed from the oil bath and allowed to cool to room temperature. When cooled, the solution was transferred to a 4-5.5 μm fine glass filter Büchner funnel set up on a 1L Erlenmeyer flask and suction filtered by using an aspirator. The filtrate was then transferred to a volumetric flask and diluted to 250 mL.

A 25 mL leachate sample was then pipetted into a beaker, and titrated with 0.1 M of HCl in a 751 GPD Titrino from Metrohm. The volume of HCl was noted and the KOH amount was calculated using Equation 3-2.

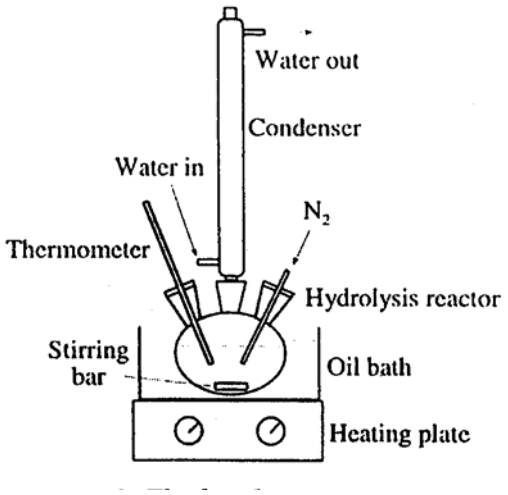

Figure 3-2. Leaching equipment.

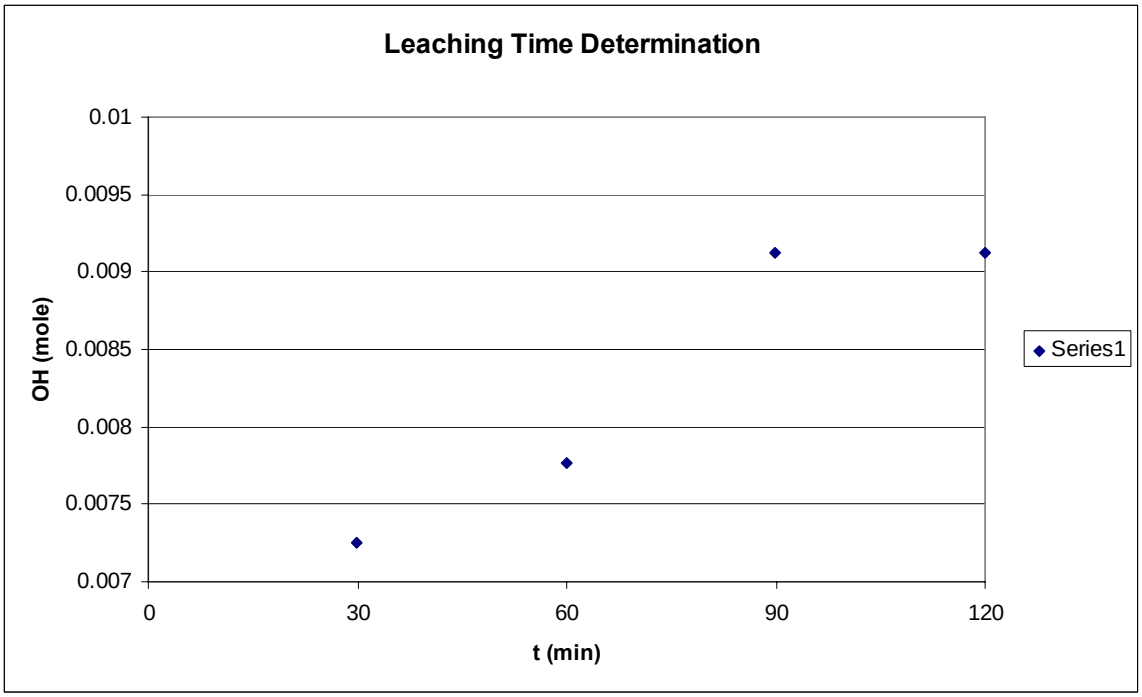

Figure 3-3. Amount of OH^- on sample collected every 30 minutes.

$$M = \frac{v * 0.1M}{25mL} * 0.025L * 10 \qquad \text{Equation 3-2}$$

Where: M = OH^- (moles)

v = Volume of HCl (mL)

3.2.4. Particle Size Measurement

The particle sizes of the sample and products were measured using Malvern 2600. The data were used to model the reaction mechanism shown in Table 1-1.

3.2.5. Carbonate Analysis

Carbonate ion was analyzed using Phase Reaction Conversion Headspace Gas Chromatography (PRC-HS-GC) technique. The sample was first injected with sulfuric acid in a vial. The vial was then shaken and heated up in a headspace sampler to produce

carbon dioxide according to Reaction 3-2. The carbon dioxide was then transferred by the sampler to a gas chromatograph to be analyzed quantitatively[18].

$$2\ H^+ + CO_3^{2-} = H_2CO_3 \rightarrow CO_2 + H_2O \qquad \text{Reaction 3-2}$$

4. Results and Discussion

Equilibrium calculations and experiments were carried out on potassium carbonate-titanium dioxide chemical system, and the results would be compared. Temperature was the only condition studied.

4.1. Equilibrium Calculation

Equilibrium calculations were performed for a temperature range of 700-950^{o}C. Four moles of potassium carbonate and five moles of titanium dioxide were used as the starting materials. The results obtained are shown in Table 4-1. Direct causticization was not accomplished because $4K_2O.5TiO_2$ was not produced. Comparison to experimental data will be discussed later.

Table 4-1. Equilibrium calculation results.

T(^{o}C)	CO_2 (g)(mol)	K_2CO_3 (mol)	$K_2O.6TiO_2$ (s) (mol)	$K_2O.3TiO_2$ (s) (mol)
700	0.833	3.167*	0.833	-
750	0.833	3.167*	0.833	-
800	1.667	2.333*	-	1.667
900	1.667	2.333*	-	1.667
925	1.667	2.333**	-	1.667
950	1.667	2.333**	-	1.667

*solid phase, **liquid phase

4.2. Rate Determining Step and Kinetic Model

Experiments were carried out at six different temperatures at least twice. The data were then averaged and standard deviations were calculated. The results are presented in Figure 4-1.

The figure shows that reaction rates and conversions increase with temperature. The increase in the reaction rates could be explained by Arrhenius' law,

Equation 1-1. However, the conversions for 925°C and 950°C are found to be the same. It might imply that the maximum conversion the reaction could go was 0.90. That the reaction did not reach completion might due to an insufficient amount of TiO_2. The possible solid products formed were $4K_2O{\cdot}5TiO_2$, and $K_2O{\cdot}3TiO_2$ (Reactions 1-9 and 1-10). According to Reaction 1-7, the formation of $K_2O{\cdot}3TiO_2$ implies 3 mole TiO_2 was consumed for every mole of K_2CO_3, while 1.25 mole TiO_2 was consumed for every mole of K_2CO_3 to form $4K_2O{\cdot}5TiO_2$. Since the starting materials were made based on $4K_2O{\cdot}5TiO2$ formation, no TiO_2 was available after certain time due to the additional formation of $K_2O{\cdot}3TiO_2$.

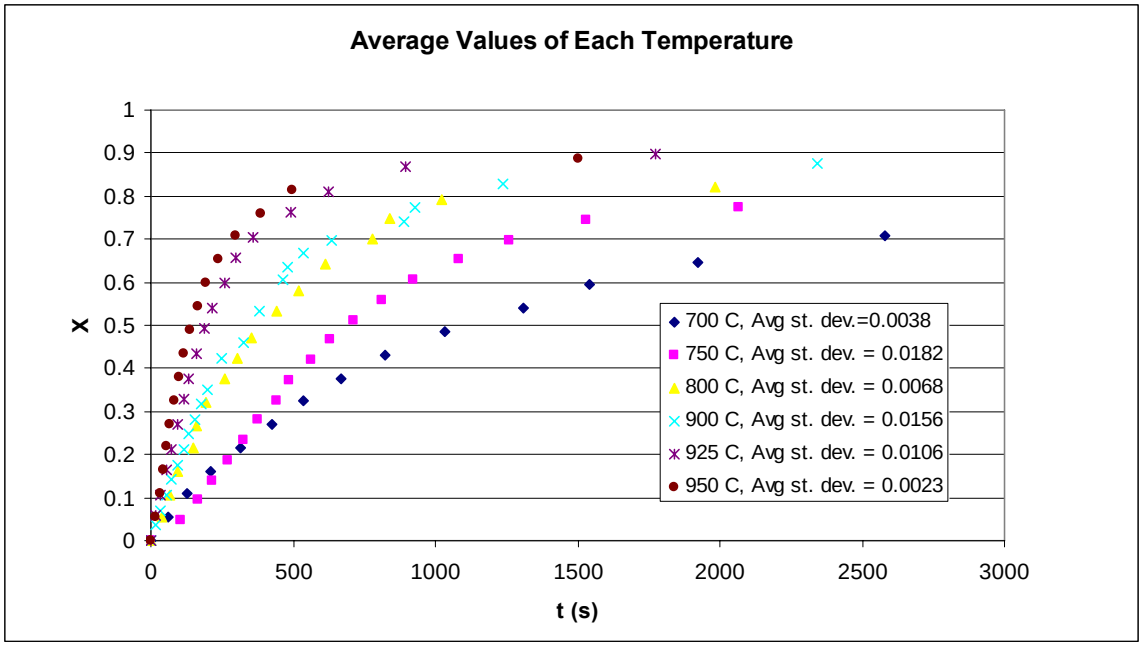

Figure 4-1. Average conversion curves at different temperatures.

Kinetic models that would be applied to the data are summarized in Tables 1-1 and 1-2. The possible rate determining steps are diffusion and kinetic control. These are determined by plotting the experimental data according to the model equations in the Tables.

By plotting time data as the X-axis and the whole terms on the right side of the equations as the Y-axis, a straight line should be drawn. A trendline was then added

which would establish its equation and R^2. The R^2 values for each model and temperature are shown in Table 4-2a.

The R^2 obtained for the whole models are in the range of 0.12 – 0.98, and a conclusion that could be drawn is the rate determining step for K_2CO_3 and TiO_2 reaction is diffusion. For the solid-solid reaction, the diffusion control models show similar R^2. However, Valensi-Carter model is chosen to describe the reaction mechanism after further analysis was done. Since the reaction might have reached equilibrium earlier than the terminated time, the last data for each temperature was eliminated and R^2 was recalculated, as shown in Table 4-2b. The Valensi-Carter model showed a better fit to the data than the other two models. For the reaction between melted potassium carbonate and titanium dioxide, ash diffusion control model was found to have the best fit.

Table 4-2a. R^2 for each model.

Model	700°C	750°C	800°C	900°C	925°C	950°C
Ginstling-Brounshtein	0.9860	0.9389	0.8721	-	-	-
Jander	0.9767	0.9286	0.8933	-	-	-
Valensi-Carter	0.9824	0.9474	0.8323	-	-	-
Reaction Control	0.9007	0.9120	0.6540	0.8805	0.4237	0.2096
Ash Diffusion Control	-	-	-	0.9738	0.7891	0.7033
Film Diffusion Control	-	-	-	0.2241	0.1233	0.4012

Table 4-2b. R^2 for each model after data adjustment.

Model	700	750	800	900	925	950
Ginstling-Brounshtein	0.9769	0.9192	0.9651	-	-	-
Jander	0.9638	0.896	0.9408	-	-	-
Valensi-Carter	0.9944	0.984	0.9938	-	-	-
Reaction Controls	0.9396	0.978	0.9625	0.9134	0.8239	0.8918
Ash Diffusion Controls	-	-	-	0.9649	0.969	0.9774
Film Diffusion Controls	-	-	-	0.6905	0.5264	0.6923

Reaction rates were obtained after the appropriate model was determined. The rates were then analyzed for their reaction constants using Arrhenius' law and recorded in Tables 4-3 and 4-4. The rates increase with temperature as expected. The information obtained from the Arrhenius' plots was then used to estimate time from the conversion

data collected during the experiments. The results are seen in Figures 4-2 to 4-7 with Figures 4-2a to 4-7a obtained after data adjustment. The model does not fit well for low conversions because the samples were inserted in the heating furnace at room temperature, and they required some time to reach the set temperature.

Table 4-3. Reaction parameters for Valensi-Carter model.

T (^oC)	k ($\mu m^2/s$)	k_o ($\mu m^2/s$)	E_a/R^* (K)	R^2
700	0.00057	1.15	7368.2	0.9649
750	0.00093			
800	0.00115			

R* = 8.314 J/(mol.K)

Table 4-4. Reaction parameters for ash diffusion controls model.

T	D/r^2 (g/mL.mol.s)	D_o/r^2 (g/mL.mol.s)	E_a/R^* (K)	R^2
900	0.01136	2.47	6356.9	0.7395
925	0.01136			
950	0.01420			

R* = 8.314 J/(mol.K)

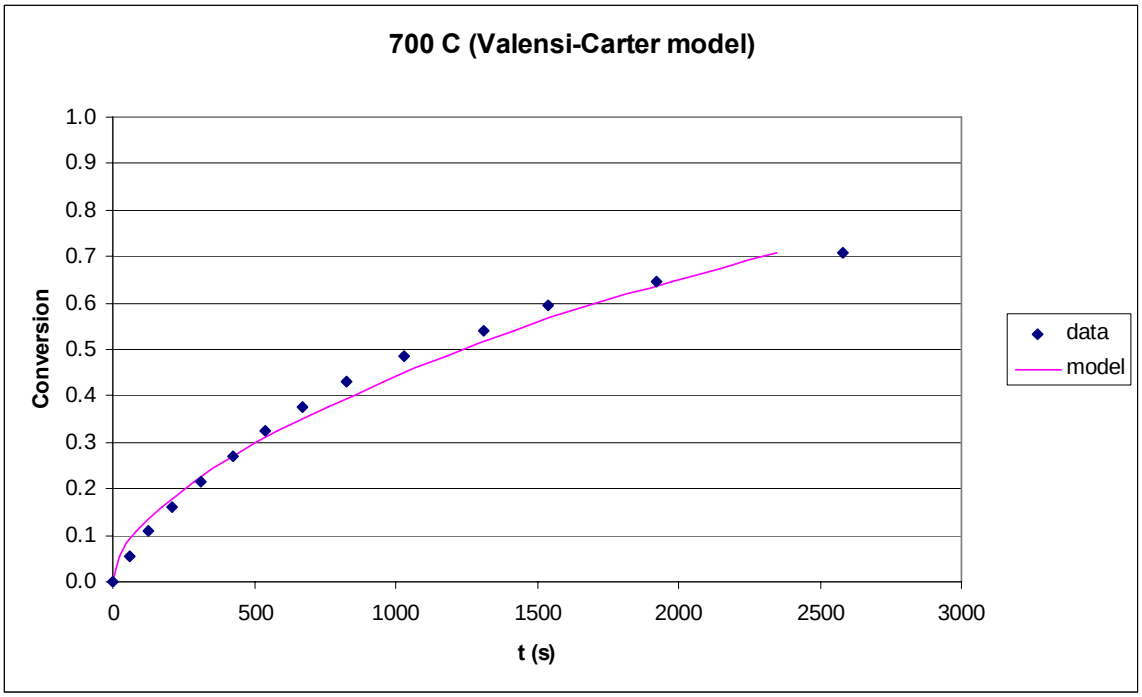

Figure 4-2. Data vs. model at 700^{o}C.

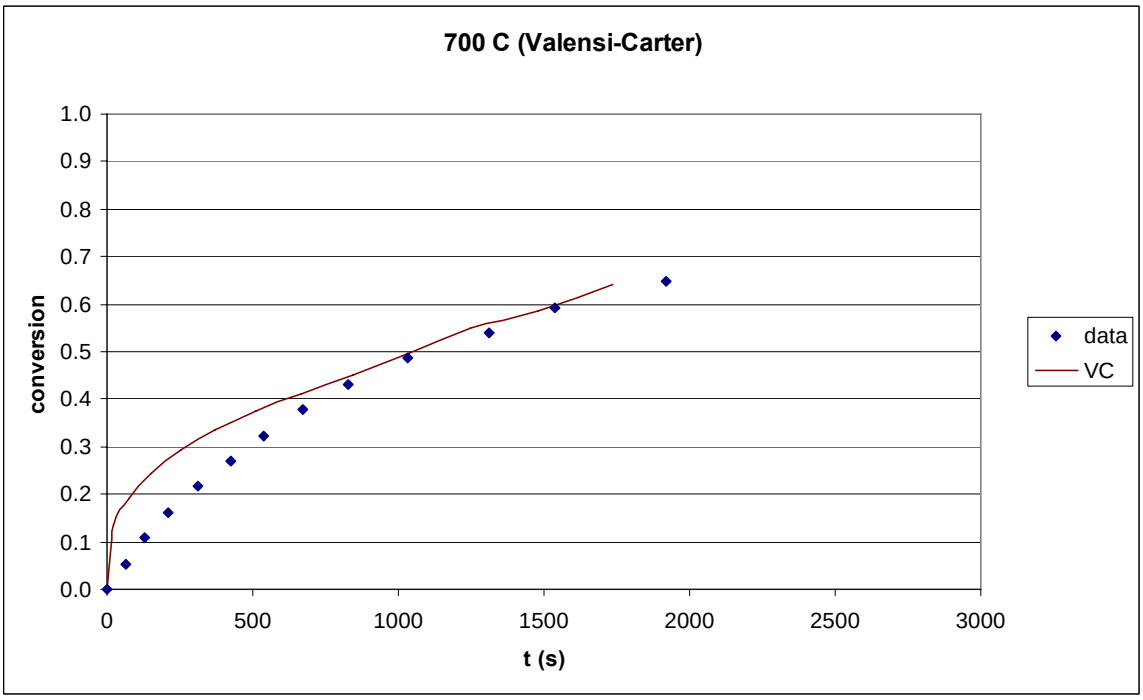

Figure 4-2a. Data vs model at 700^{o}C after data adjustment.

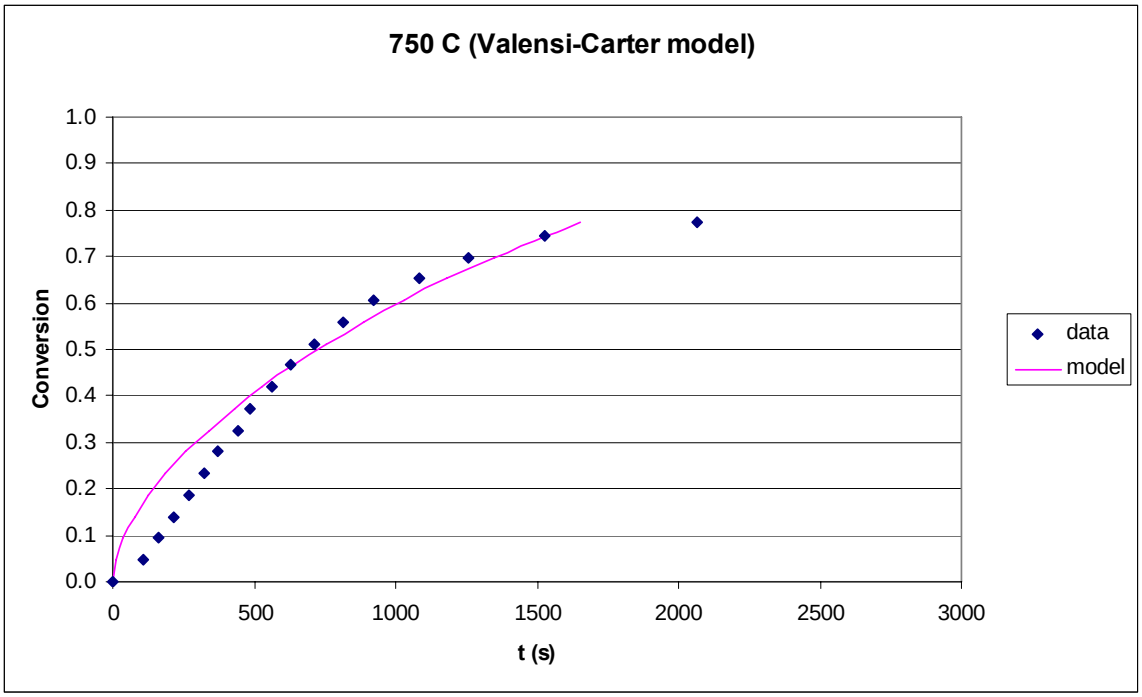

Figure 4-3. Data vs. model at 750^{o}C.

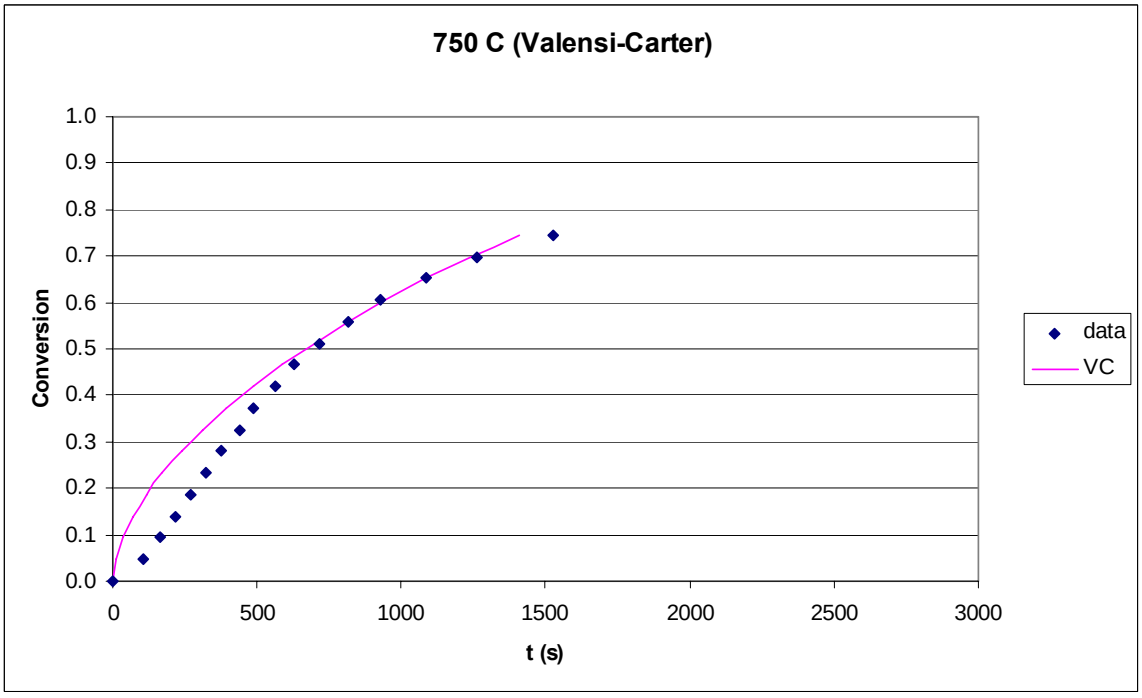

Figure 4-3a. Data vs model at 750^{o}C after data adjustment.

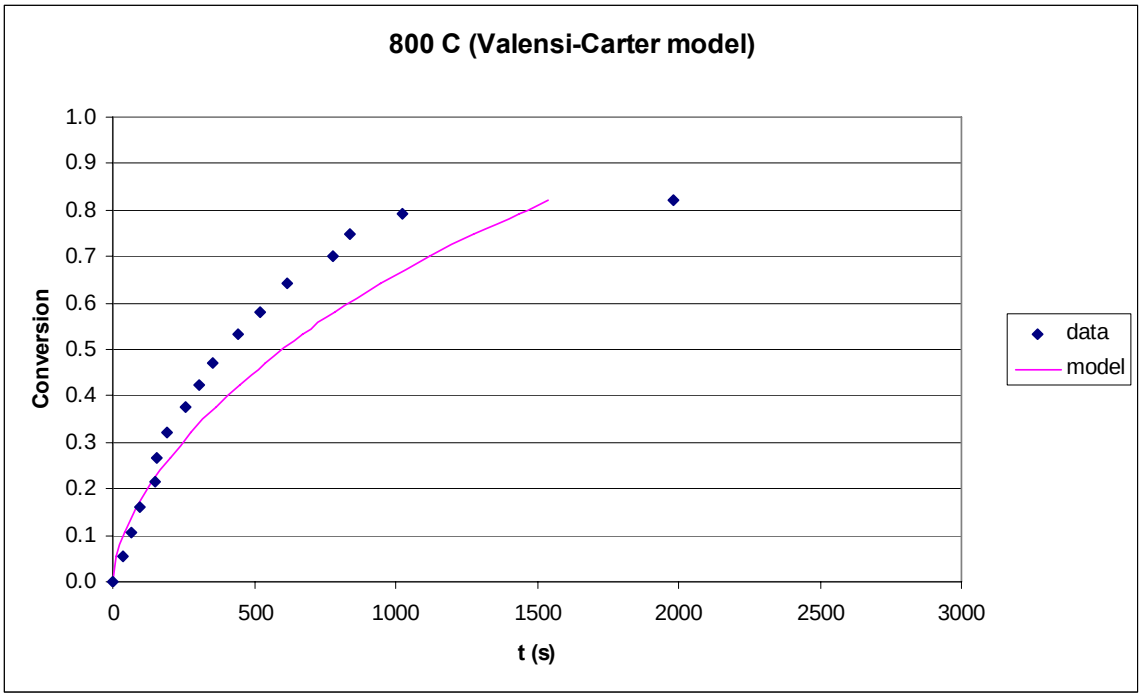

Figure 4-4. Data vs. model at 800^{o}C.

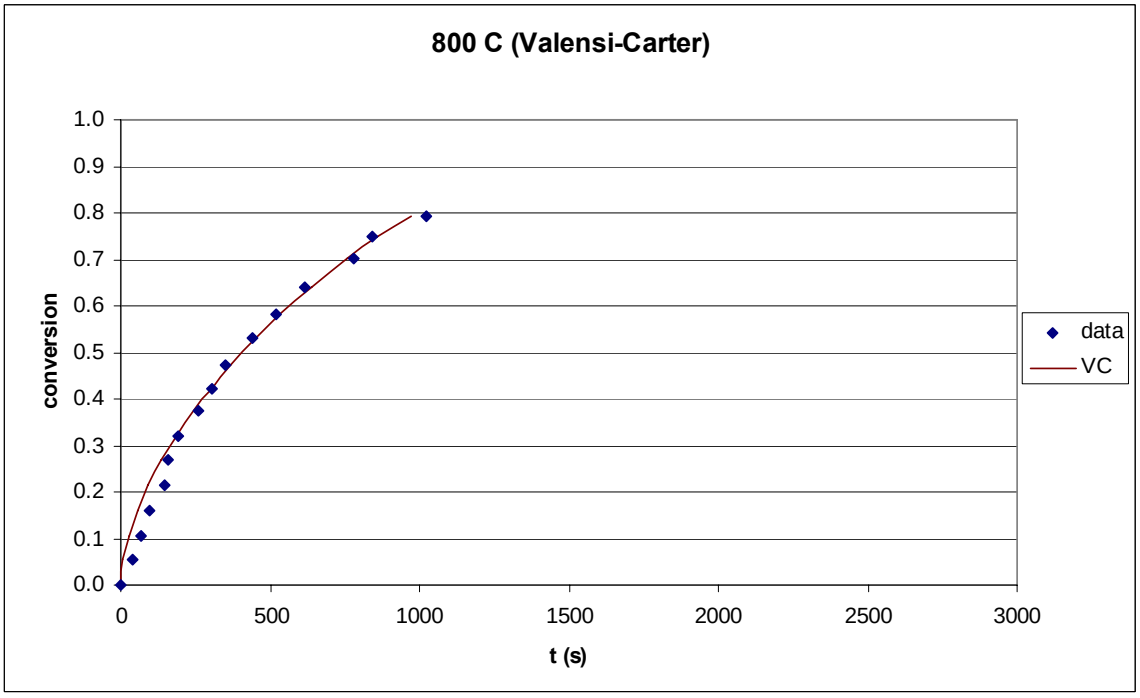

Figure 4-4a. Data vs model at 800^{o}C after data adjustment.

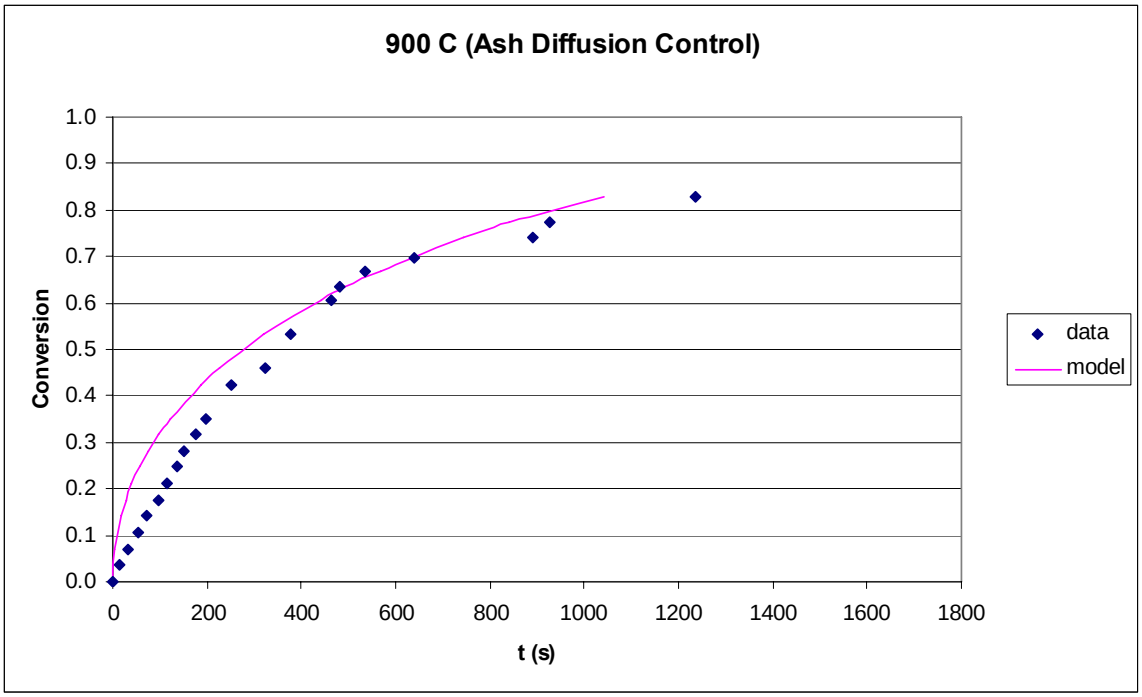

Figure 4-5. Data vs. model at 900^{o}C.

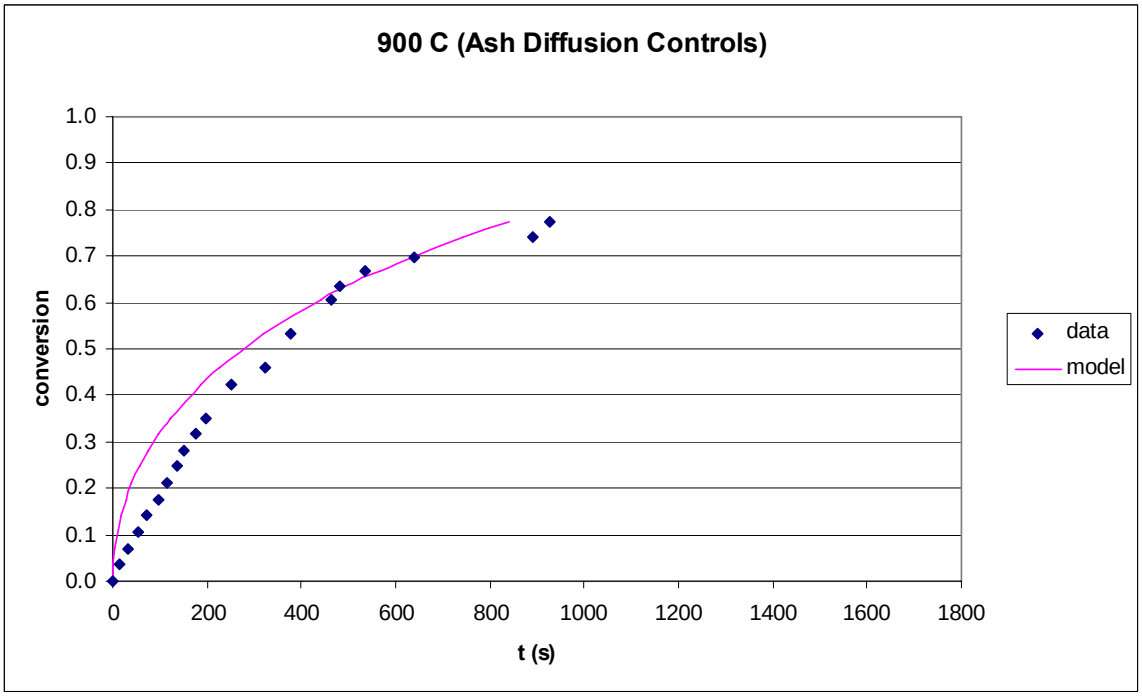

Figure 4-5a. Data vs model at 900^{o}C after data adjustment.

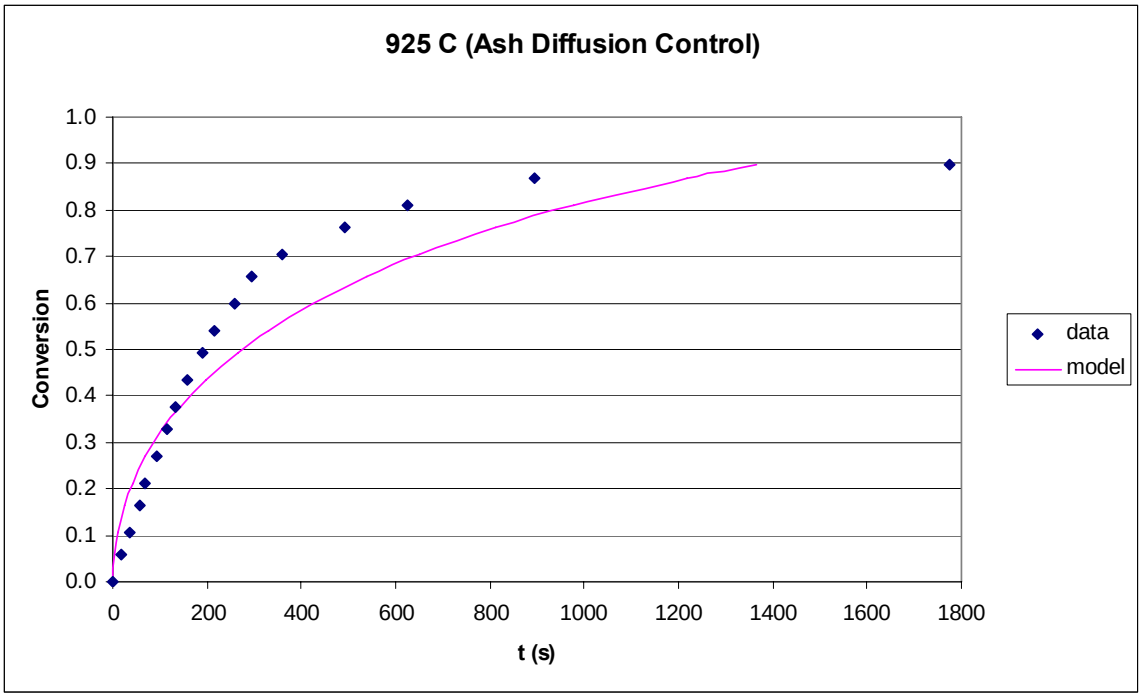

Figure 4-6. Data vs. model at 925^{o}C.

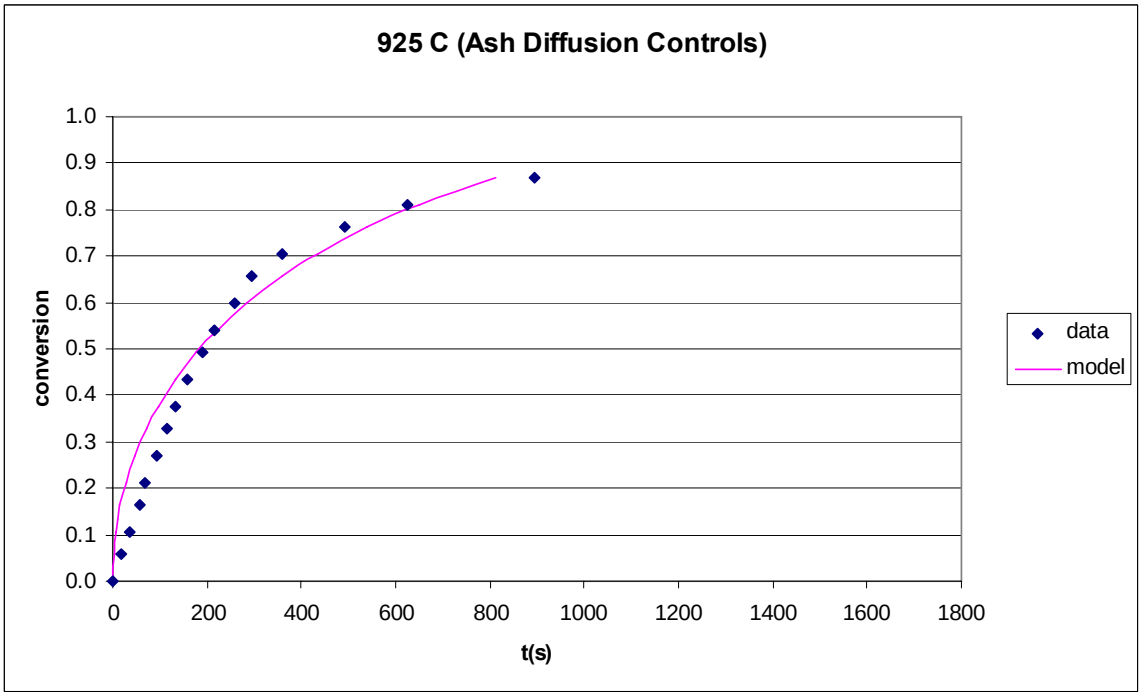

Figure 4-6a. Data vs model at 925^{o}C after data adjustment.

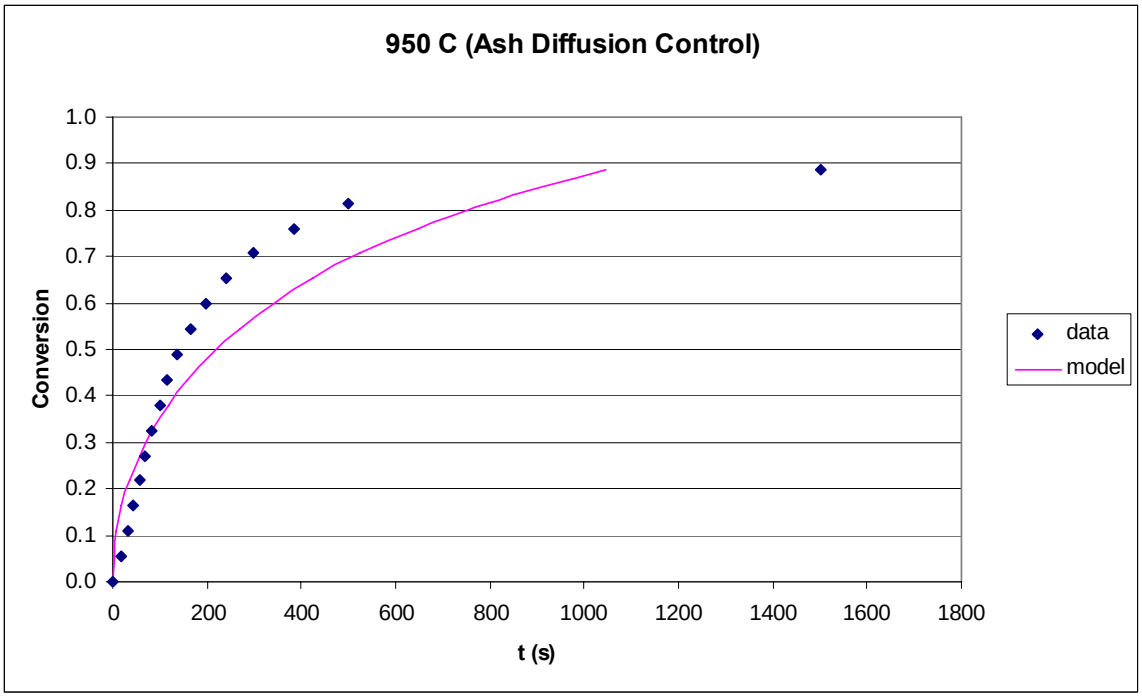

Figure 4-7. Data vs. model at 950°C.

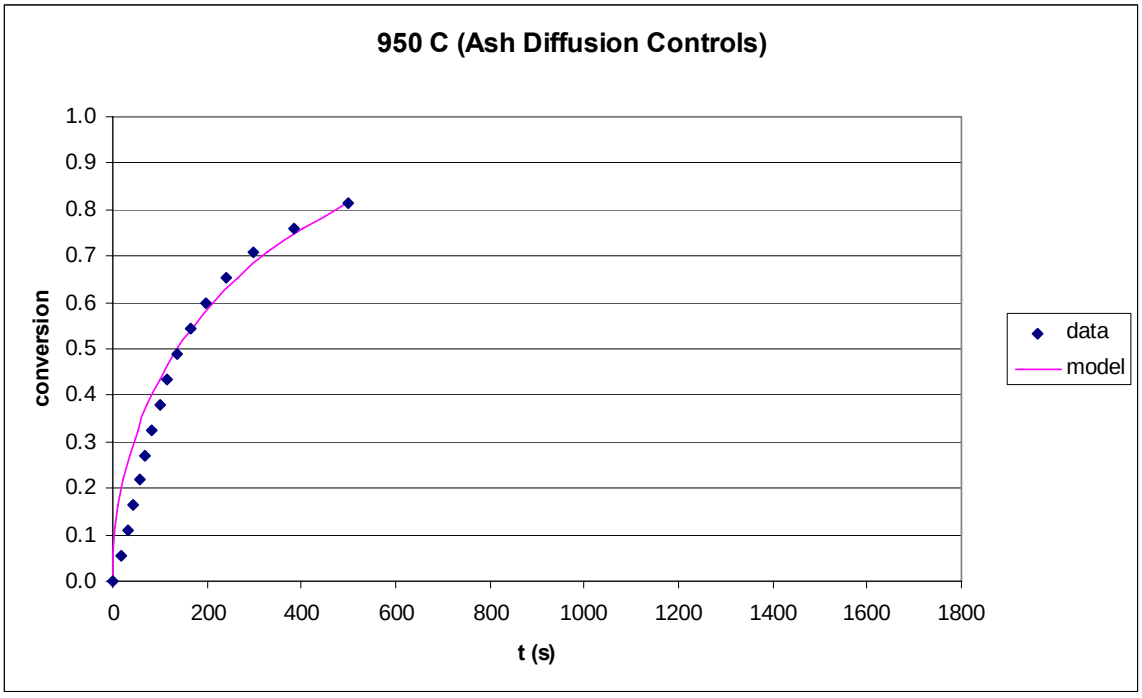

Figure 4-7a. Data vs model at 950°C after data adjustment.

4.3. Leaching

$4K_2O{\cdot}5TiO_2$ was expected to form as the final product from the previous high temperature experiments. The product was then leached with water to convert it to KOH to confirm the $4K_2O{\cdot}5TiO_2$ formation. The amount of KOH was measured by titrating the solution with HCl at least three times and the results are presented in Figure 4-8. The amount of KOH increases as temperature increases which is consistent with the fact that at higher temperatures, higher conversions were obtained (refer to Figure 4-1); therefore, more $4K_2O{\cdot}5TiO_2$ was formed during the reaction.

The KOH values overlap with each other for some temperatures. Calculations for the KOH formation assumed that 25.0mL of the leachate was titrated. However, pipetting the leachate to be exact was difficult. A difference in 0.5mL might cause the data to change by 0.00008-0.0001 mol. Therefore, the titration was carried out at least three times for each sample.

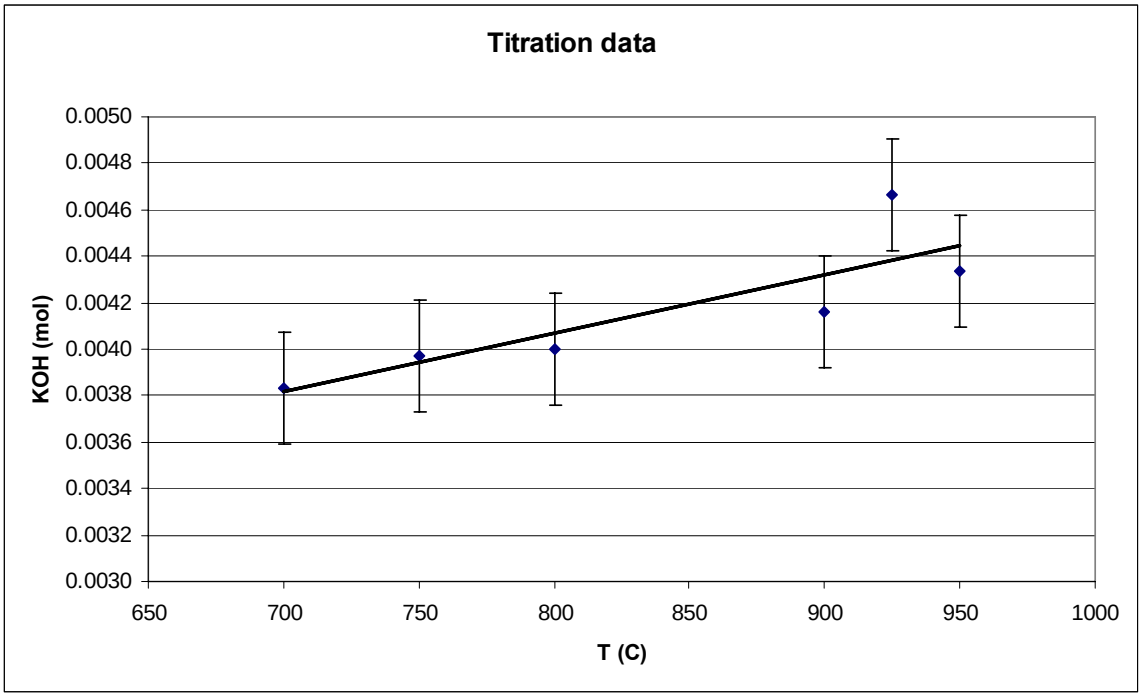

Figure 4-8. KOH amount at different temperatures.

4.4.Data Comparison

The FactSage5.1 data has shown that no $4K_2O{\cdot}5TiO_2$ is formed at equilibrium; therefore, direct causticization is not achieved. However, by analyzing leaching results, the presence of $4K_2O{\cdot}5TiO_2$ could be confirmed, as shown in Figure 4-8.

The thermodynamic data for some of the chemicals in the FactSage5.1 might need further investigation because some values are different from another source. For example, the melting points of Na_2CO_3 and K_2CO_3 are listed as 858°C and 901°C, respectively. But values of 851°C (Na_2CO_3) and 891°C (K_2CO_3) are obtained from Perry's Handbook [19]. Also, the thermodynamic data for $4K_2O{\cdot}5TiO_2$ is good for up to 904°C only according to the database.

4.5. Carbonate Analysis

In addition to leaching, products from the high temperature experiments were analyzed for their carbonate content using the method described in previous section. The GC results and estimated carbonate contents obtained from Figure 4-1 are presented in Table 4-5. The carbonate content decreases as temperature increases because higher conversions were obtained at higher temperatures. However, data for 950°C from the GC does not follow the trend. It might due to unknown experimental errors because of two reasons:

1. The carbonate content should be around 0.100 g/g as estimated from Figure 4-1 because 0.90 conversion was achieved during the high temperature experiments.
2. Leaching results revealed that 950°C had a higher KOH content than samples from temperatures below 900°C. Therefore, a low carbonate left in the 950°C sample was expected.

Table 4-5. Carbonate Content Obtained from GC and Figure 4-1.

Temperature (°C)	Carbonate from GC (g/g)	Carbonate from Figure 4-1 (g/g)
700	0.298	0.291
750	0.232	0.227
800	0.217	0.180
900	0.150	0.123
925	0.138	0.103
950	0.254	0.114

5. Conclusions

The purpose of this study was to model the kinetics of direct causticization using titanium dioxide in a potassium-based chemical instead of sodium. The modeling was accomplished using available models that had been developed by others.

Reactions of K_2CO_3 and TiO_2 were run at six different temperatures. Higher rates and conversions were achieved at higher temperatures as expected. The highest conversion was around 0.90. Full conversion could not be obtained due to the limited amount of TiO_2.

Modeling the kinetics had shown that the reaction is diffusion limited. The Valensi-Carter model had shown a good fit for a temperature range of 700-800^{o}C, while ash diffusion control was chosen for the higher temperatures.

Leaching experiments were performed to measure how much KOH was formed from the heated samples. An increasing trend was observed as temperature was increased. The data was then compared to the FactSage© data. An opposite observation was obtained. The leaching results confirmed that $4K_2O{\cdot}5TiO_2$ was actually formed.

6. Recommendations for Future Work

1. Run experiments using $K_2O \cdot 3TiO_2$ instead of TiO_2 as the initial reactant.
2. Collect solid product from the leaching experiment to measure how much $K_2O \cdot 3TiO_2$ formed.
3. Develop a model that could fit at all conversions.
4. Record data in a smaller weight loss increment especially when the reaction almost reaches equilibrium.

7. Acknowledgment

I would like to thank to the following individuals who made this project successful:

1. Dr. Jeff Empie
2. Dr. Preet Singh
3. Dr. Scott Singuefield
4. Dr. Ingrid Nohlgren
5. Dr. Xin-Sheng Chai
6. Dr. Mike Buchanan
7. Xiaoyan Zeng
8. Alan Ball
9. Daniel Gershon
10. Pablo Conde

8. References

1. Grace, T.M., "Can Kraft Mills be Pottasium-based," PIMA Magazine, 76(6), 82-83, 1994.
2. Richardson, B., et. al., "Behaviour of Non-Process Elements in the Kraft Recovery System," 1998 International Chemical Recovery Conference, pp 1025- 1039.
3. Green, R.P., and Hough, G., *Chemical Recovery in the Alkaline Pulping Process*, 3rd ed., TAPPI Press, 1992.
4. Salmenoja, K., "Achievements in the Control of Superheater Corrosion in Black Liquor Recovery Boilers".
5. Hill, E.S., "Potassium based pulping in closed mills," A190 Final Report, IPST, Atlanta, GA, 1996
6. Grace, T.M. and Timmer, W.M., (1995), "A Comparison of Alternative Black Liquor Recovery Technology," *1995 International Chemical Recovery Conference*, Toronto, Ont., April 26-27, p. B269-B275.
7. Kiiskilä, E. (1979a), "Recovery of Sodium Hydroxide from Alkaline Pulping Liquors by Smelt Causticizing, Part II, Reactions between Sodium Carbonate and Titanium Dioxide," *Paperi ja Puu - Papper och Trä*, 61(5), p.394-401.
8. Kiiskilä, E. (1979b), "Recovery of Sodium Hydroxide from Alkaline Pulping Liquors by Smelt Causticizing, Part III, Alkali distribution in titanium dioxide causticizing," *Paperi ja Puu - Papper och Trä*, 61(6), p.453-464.
9. Kiiskilä, E. and VALKONEN., N., (1979c), "Recovery of Sodium Hydroxide from Alkaline Pulping Liquors by Smelt Causticizing, Part IV, Causticizing of Sodium Carbonate with Ferric Oxide," *Paperi ja Puu - Papper och Trä*, **61**(8), p. 505-510.
10. Kiiskilä, E. (1979d), "Recovery of Sodium Hydroxide from Alkaline Pulping Liquors by Smelt Causticizing, Part V, Causticizing of Molten Sodium Carbonate with Ilmenite," *Paperi ja Puu - Papper och Trä*, 61(9), p.564-577.
11. Nohlgren, I., "Recovery of Kraft Black Liquor with Direct Causticization using Titanates," Ph.D. Thesis, Luleå University of Technology, Luleå, Sweden (2002).
12. Eames, D.E. and Empie, H.J., "Direct Causticizing of Sodium Carbonate with Manganese Oxide," NPPRJ 17(4), 369 (2002).

13. Zou, X., Kubes, G.J., Van Heiningen, A.R.P. and Avedesian, M.M., "Autocausticizing of Kraft Black Liquor:Process Implications Based on Chemical Equilibrium Calculations," Pulping Conference, 1990.

14. Levenspiel, O., Chemical Reaction Engineering, 3rd edition, 1999.

15. Tamhakar, S.S. and Doraiswamy, L.K., "Analysis of Solid-Solid Reactions: A Review," *AICHE J.,* 1979, 25(4), p. 561-582.

16. Carter, R.E., "Kinetic Model for Solid-Solid Reactions," *J. Chem. Phys*., 1961, 34(6), p. 2010-2015.

17. www.chemfinder.com

18. Chai, X.S., et al., "Analysis of Nonvolatile Species in a Complex Matrix by Headspace Gas Chromatography," *Journal of Chromatography*, 2001.

19. Perry, R.H., and Green, D.W., Perry's Chemical Engineers' Handbook, 7th ed, 1997.